Plasticizing effect of oxidized biodiesel on polyethylene observed by nondestructive method

A.K. Saad, F.P.C. Gomes, M.R. Thompson*

Department of Chemical Engineering, CAPPA-D/MMRI

McMaster University, Hamilton, Ontario, Canada

Published manuscript at Fuel ©Elsevier

DOI: 10.1016/j.fuel.2019.04.122

Abstract

This paper explores the compatibility of biodiesel with different grades of polyethylene, specifically examining the extent of plasticization in order to gain a better understanding of the biofuel's compatibility with this common polymer. Its bulk influences on polyethylene were investigated by gravimetric and mechanical testing, and by the application of a newly developed nondestructive ultrasonic testing method. Diffusion rates and the extent of plasticization by biodiesel were compared to results obtained with toluene, a known plasticizer for polyethylene. Mechanical and gravimetric analysis showed that biodiesel exhibited bulk attributes of a plasticizer for the tested polyethylenes with reduced moduli proportional to the amount of fuel uptake and that uptake was inversely proportional to crystalline content of the polymer. Based on uptake amounts, the efficiency of biodiesel as a plasticizer towards polyethylene was found to be more than double that of toluene. However, spectral analysis by ultrasonics showed that absorbed toluene and biodiesel influenced the microstructure of polyethylene differently. Notable differences in internal stresses were noted between the two fluids for the same amount absorbed. A subsequent study analyzed the impact that biodiesel degradation had on plasticization. Although the trend showed a slight change in diffusion rate with increasing oxidation of the medium, the mechanical and ultrasonic results did not show significant differences between fresh and degraded biodiesel within the 45 days span of the test. Combining the evidence observed in this study, a mechanism is proposed for biodiesel plasticization that can help with failure prevention and material selection.

Keywords: Compatibility; Ultrasonic Testing; Ageing; Toluene.

3.1. Introduction

The use of polymers in parts design that will be exposed to chemicals always generates routine compatibility concerns. Thus, designers require proper identification of any chemical and physical interactions that would undermine the functionality of a manufactured part. Polyethylene (PE) is a common material used for chemicals storage including fuel tanks in automobiles, marine vessels and agricultural machinery [1]. Recently, biodiesel has emerged as a viable bio-sourced fuel alternative to fossil fuels, presently blended at low fractions with diesel, making it a relevant compatibility concern for polyethylene fuel tanks. Most of the biodiesel compatibility studies on polymers other than polyethylene have focused on elastomers, which reported swelling with a corresponding decline in mechanical properties [2,3]. A few recent studies on polyethylene [4-11] have suggested interactions with biodiesel may be quite aggressive.

A small number of long-term compatibility studies with biodiesel have reported swelling with notable weight gains and discoloration of high density polyethylene (HDPE) [4,7-9,11]. Several of these studies [8,9,11] reported on the plasticizing nature of biodiesel, shown by a marked decrease of Young's Modulus and increase of the stain-at-max stress, which was related to the concentration of absorbed fuel in the polymer. Relevant factors affecting absorption of biodiesel into polyethylene, such as the polymer crystalline morphology and changes in biodiesel chemistry due to degradation have not yet been studied. However, related studies have shown fatty acids and vegetable oils to be effective plasticizers in different polymers and rubbers [12-17].

An often overlooked shortcoming of biodiesel in compatibility testing is its changing chemical and physical properties associated with oxidation. Biodiesel is susceptible to degradation and does so more rapidly with heating, generating several by-products including free fatty acids [11,18-20]. Some studies [7,11] have found no effect of biodiesel degradation on polyethylene,

chemically, over more than a year of observation while others [9,10,21,22] reported accelerated oxidative degradation of polyethylene by the formed unsaturated fatty acids during aging. The differences may be attributed to the different testing environments in these studies. Whether those degradation products of biodiesel exhibit differing absorption and plasticization effects on polyethylene has yet to be considered.

External plasticization of polyethylene is commonly correlated with the diffusion of penetrants over a certain exposure time that can be monitored either gravimetrically or by analysis of mechanical properties [23]. The latter is more definitive, since mass changes may be difficult to detect, though it is considered a destructive characterization method and that is often undesirable. Nuclear magnetic resonance (NMR) has been applied to evaluate the penetration of solvents into different morphologies of polyethylene, showing diffusion on the amorphous phase, but this approach would also fall under the destructive category of evaluations [24]. Few nondestructive characterization techniques exist for this characterization; most of them are focused on spectroscopic analysis. Infrared spectroscopy can track the penetration of small molecules by their chemical constituents through thin films [25] and at the surface of thicker objects [26]. But in this case, the analysis is limited to a small, localized region and is incapable of making a bulk characterization of plasticization in polymer samples. Nonlinear ultrasonic testing has been shown as a promising technique to evaluate the penetration of small molecules in polyethylene, give a bulk assessment of internal stresses and modifications to the semi-crystalline structure of HDPE by observing spectroscopic variations [27].

In this paper, a newly developed non-destructive characterization technique based on nonlinear ultrasonics is compared to gravimetric and mechanical analyses to study the effects of biodiesel on different grades of polyethylene. The plasticizing ability of biodiesel will be studied

relative to toluene, as a known plasticizer and will consider the impact of biodiesel ageing. The study results are meant to improve material compatibility libraries for part design involving exposure to this new biofuel.

3.2. Materials and methods

3.2.1. Materials

Four grades of polyethylene covering a wide range of properties were used. Three of the resins were HDPE grades, denoted with the prefix HD, while the fourth resin was a linear low density (LLDPE) grade, denoted with the prefix LL. The numbers after each prefix (HD and LL) refer to the polyethylene grade named by the vendor. The materials were provided by Imperial Oil Ltd (Sarnia, ON) in pellet form. A summary of properties can be found in Table 3.1, with data provided from the supplier. The polymer pellets were compression molded according to Procedure C of Annex 1 in ASTM D4703 and were cut into rectangular strips of dimensions 125 mm x 20 mm x 3 mm (thickness) for absorption and tensile tests.

Table 3.1. Summary of key properties of all resins used in the experimental work.

Reference Code	Density (g/cm^3)	MFI (g/10min)*
HD 8660.29	0.941	2.0
LL 8460.29	0.938	3.3
HD 6605.70	0.948	5.0
HD 6719.17	0.952	19

* MFI = melt flow index, measured according to ASTM D1238.

Biodiesel, a tallow-based methyl ester prepared from animal renderings, was generously provided by Rothsay Biodiesel Inc (Guelph, ON) in pure form (B100). The biodiesel was stored in a deep freezer at a temperature of -40 ºC till used for testing. The mentioned degraded biodiesel in the study was obtained by accelerated oxidation, heating it at 50 ℃ for 45 days immediately prior to testing. Toluene was obtained from Caledon Laboratories (ON, Canada).

3.2.2. Preparation of plasticized samples

Rectangular-cut specimens of each resin grade were placed in a test tube with fresh or degraded biodiesel and placed in a hot water bath (VWR Corporation) at 50 ºC for up to 45 days and their weights were measured daily to track the diffusion of biodiesel in to the samples. Fluid absorption was measured gravimetrically for three replicates of each grade with a Mettler Toledo AE200 Analytical Balance. Surfaces were wiped (dried) using paper towels before the measurements were taken. The concentration of absorbed biodiesel in the samples was given as a percent increase in mass. As a means of comparison, the same grades of polyethylene were also plasticized with toluene. With higher sorption properties in polyethylene, samples only needed to be prepared at 25 ºC with toluene to reach comparable uptake concentrations to those achieved with biodiesel for the subsequent analysis of properties.

3.2.3. Mechanical properties

Tensile tests were performed on notched rectangular strips. For the rectangular samples, two side notches of 2 mm depth were applied along the center-line using single-side sharped razor blades (VWR Corporation). Tests were executed in a universal mechanical testing system (Instron Corporation Model 3366) with a 5 kN load cell, at a cross-head speed of 35 mm/min. Results from tensile tests were based on three samples for each grades tested.

3.2.4. Ultrasonic testing

A physical non-destructive characterization of the plasticized samples was done through nonlinear ultrasonic testing. The following procedure was described in previous work [27]. Two ultrasonic transducers (Physical Acoustic Corporation, NJ) were coupled to the surface of the specimen using high vacuum grease (Dow Corning), with a center-to-center separation of 35 mm. The emitter (model R15) had a resonant frequency at 150 kHz whereas a broadband sensor (model F30a) was used for the receiver. Emitted ultrasonic pulses were produced at frequencies from 135 to 165 kHz in 1 kHz step increments, with the corresponding received signals recorded at an acquisition rate of 4 MHz and processed using a combination of a LabView and Python codes. A nonlinear 'ultrasonic parameter' was calculated from the ratio between the amplitude of third harmonic peak (A_3) over the amplitude at the primary emitted frequency (A_1).

3.2.5. Biodiesel characterization

The acid number was determined following ASTM D974 to track the extent of oxidation in the degrading fuel. For good sensitivity at low acidity values, a 0.01 N standardized KOH solution (Sigma-Aldrich) was used for the titrations. The endpoint was detected using phenolphthalein as an indicator. Tests were done in triplicates.

Surface tension was measured for pure fresh and pure degraded biodiesel using the pendant drop method by means of a 90º blunt end tip needle with a diameter of 1.27 mm. Twenty-six images, spaced 2 seconds apart, were taken for each drop by a digital camera acting as a goniometer and processed for their shape using an image analysis software (Kruss).

Viscosity of the fresh and degraded biodiesel was measured using a Discovery DHR-2 parallel plate rheometer (TA Instruments). A frequency sweep spanning 0.1–200 rad/s was performed at a temperature of 25℃ with a resolution of 5 points per decade. A Newtonian fit curve

was provided at the end of the test, which was used to compute the viscosity of the biodiesel samples. The test was completed for three replicates of each fluid.

3.3. Results and discussion

3.3.1. Differences in absorption between biodiesel and toluene

In the preparation of biodiesel plasticized polyethylene specimens, their weight gains were monitored to assess absorption rate differences as well as final uptake between the different grades of polyethylene. Figure 3.1 shows the typical percent weight gain for the four polyethylene grades plotted against immersion time in fresh B100 biodiesel.

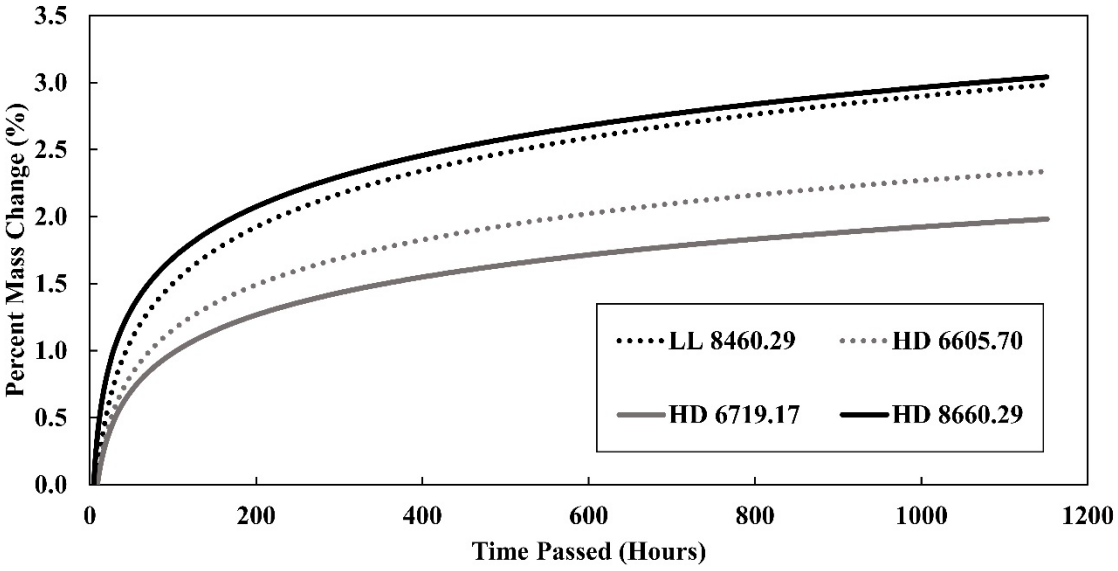

Figure 3.1. A plot of average percent weight change (%) vs. time passed (hours) in biodiesel of HD 8660.29 (black solid line), LL 8460.29 (black dotted line), HD 6605.70 (gray dashed line), and HD 6719.17 samples (gray solid line). Experimental data points were fitted with a logarithmic curve. The logarithmic curves were picked as they best represented the initial stages of the diffusion. The average R^2 value for all four grades is 0.73 depicting a good correlation.

The curves indicate that the samples had not fully equilibrated after 45 days but the trends shown suggest little further weight gains would be expected. Visual examination of the polymer samples after immersion showed distinctive yellow staining in comparison to their white appearance originally or after immersion in toluene. Faster absorption and ultimately greater fuel uptake was seen with the lower crystallinity/lower density polyethylene grades. HD 8660.29 showed a percent mass gain of approximately 3.04±0.07% over 45 days of immersion, followed by LL 8460.29 (2.98±0.02%), HD 6605.70 (2.34±0.03%) and finally HD 6719.17 with the lowest percent mass gain of approximately 1.98±0.01%; the lower densities associated with HD 8660.29 (0.941 g/cm^3) and LL 8460.29 (0.938 g/cm^3) in comparison to the other two grades exemplifies their lower crystallinity. Estimated diffusivity coefficients for a one-dimensional finite slab model (given in Table 3.2) were obtained by fitting the weight gain data with the first four terms of the power series described in Equation 1, below:

$$\frac{M_t}{M_\infty} = 1 - \frac{8}{\pi^2}\sum_{n=0}^{\infty}\frac{1}{(2n+1)^2}\exp\left(\frac{-D(2n+1)^2\pi^2 t}{l^2}\right) \qquad (1)$$

where M_t represents the mass uptake of biodiesel into the polyethylene slab up to time *t;* M_∞ denotes the equilibrium mass uptake; *D* is the diffusivity coefficient; and *l* is the thickness of the slab. Comparing diffusivity coefficients to the density of each polymer grade (given in Table 3.1), it appears that an inverse correlation exists.

Table 3.2. Diffusivity coefficients for biodiesel and toluene in LL 8460.29, HD 8660.29, HD 6605.70, and HD 6719.17.

Sample	Diffusivity of Samples in Biodiesel at 50°C [$\frac{m^2}{hours}$]	Diffusivity of Samples in Toluene at 25°C [$\frac{m^2}{hours}$]
HD 8660.29	$(17.8 \cdot 10^{-10}) \pm (0.566 \cdot 10^{-10})$	$(1.97 \cdot 10^{-6}) \pm (0.673 \cdot 10^{-6})$
LL 8460.29	$(14.0 \cdot 10^{-10}) \pm (0.702 \cdot 10^{-10})$	$(2.40 \cdot 10^{-6}) \pm (0.436 \cdot 10^{-6})$
HD 6605.70	$(9.74 \cdot 10^{-10}) \pm (1.04 \cdot 10^{-10})$	$(1.73 \cdot 10^{-6}) \pm (0.196 \cdot 10^{-6})$
HD 6719.17	$(9.21 \cdot 10^{-10}) \pm (0.938 \cdot 10^{-10})$	$(1.74 \cdot 10^{-6}) \pm (0.192 \cdot 10^{-6})$

The lower density grades, LL 8460.29 and HD 8660.29, have fitted coefficients approximately 30-45% higher than the higher density grades (HD 6605.70 and HD 6719.17), depicting a higher rate of diffusion of biodiesel into these polyethylene grades. In terms according to Cohen and Turnbull theory [4, 28], the higher diffusivity coefficient arises in LL 8460.29 and HD 8660.29 (Table 3.2) due to their larger free volume (V_f) on account of their greater amorphous content in comparison to HD 6605.70 and HD 6719.17. In other words, PE grades with higher crystalline content were less permeable to the diffusion of biodiesel, presenting a more tortuous path for the absorbed biofuel to accumulate in the amorphous regions of the polymer.

In order to compare plasticizing properties under mechanical and acoustic testing, samples were also prepared with a known plasticizer, toluene, which is a smaller molecule than biodiesel. To achieve a similar mass gain, immersion of polyethylene samples in toluene had to be done at a lower temperature in order to prevent samples from being distorted (data not shown); despite the lower ambient temperature (25 ^{o}C), its absorption rates in Table 3.2 were faster than found for biodiesel at 50 ^{o}C. The estimated diffusivity coefficients for toluene with all PE grades, included in Table 3.2, showed a similar trend but with values more than a 100% larger than those with biodiesel, depicting a much faster absorption rate into the samples. The final uptake of toluene for the different grades was highest for LL 8460.29 (4.27±0.39%). HD 8660.29 (3.83±0.23%) had a final uptake amount that is approximately 11% lower than LL 8460.29, HD 6605.70 (2.99±0.03%) and HD 6719.19 (3.07±0.08%) were approximately 43% and 39% lower, respectively. As seen by the values, the final uptake of toluene was slightly different among the grades compared to biodiesel uptake, though the larger difference due to density was consistent. This difference was due to the higher diffusion rate of toluene; and the focus of this test is to reach the closest comparable uptake of solvents for material characterization rather than finding the final equilibrium value.

3.3.2. Plasticization observed by traditional and nondestructive methods

Figure 3.2 shows the influence of the absorbed biodiesel and toluene on the mechanical properties of the polyethylene grades, following a traditional method for quantifying plasticization.

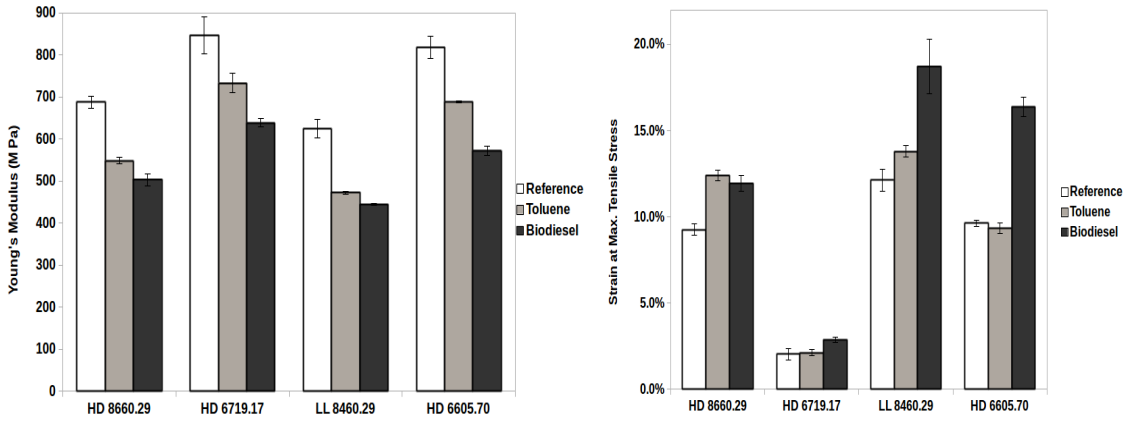

Figure 3.2. a) (Left) Summary of the elastic modulus of grades HD 8660.29, HD 6719.17, LL 8460.29, and HD 6605.70 in reference (white), toluene (gray), and biodiesel (black). Error bars represent the standard deviation of the three samples tested for each grade. **b)** (Right) Summary of the strain at max stress of grades HD 8660.29, HD 6719.17, LL 8460.29, and HD 6605.70 in reference (white), toluene (gray), and biodiesel (black). Error bars represent the standard deviation of the three samples tested for each grade.

The properties shown include Young's modulus and the strain-at-max stress of all polyethylene grades, respectively. The decline in modulus, for both fluids, shows that biodiesel shared attributes of a plasticizer in polyethylene, increasing chain mobility and reducing the secondary forces such as hydrogen bonding and Van der Waals forces between polymer chains [29]. The results show that the extent of change in mechanical properties by biodiesel is proportional to the amount of mass uptake. Samples with higher mass uptake (HD 8660.29 and LL 8460.29), showed a larger reduction in Young's modulus and greater increase in the strain at max stress. It is known that free volume possesses an inverse relationship with the rigidity of the polymer. Hence, as the free volume of the polymer is increased with increasing plasticizer concentration, the mobility of the polymer molecules also increases, making the polymer rubbery

and soft. This loss of rigidity and increase in mobility is witnessed by the decrease in the elastic modulus and the increase in the strain at max stress.

In the face of differing absorbed content in the polymer at the time of the mechanical testing, a model was necessary to compare the plasticizing influence of biodiesel to toluene on polyethylene. The model of Sothornvit and Krochta [30] was chosen to compare and quantify the effects of plasticizer composition, size, and shape on the mechanical properties of a sample. They reported being able to successfully consider three different approaches to quantify the plasticizing influence and in all cases, found an exponential dependency on the elastic modulus (*EM*):

$$EM = EM_0 \cdot e^{-x \cdot k_{EM}} \quad (2)$$

where EM_0 value reflects the original modulus of the polymer in the absence of a plasticizer; k_{EM} reflects the plasticizing efficiency of a penetrant; and x is the plasticizer content. The first approach of Sothornvit and Krochta was used in this study, quantifying the change in modulus based on the mass of absorbed plasticizer per mass of PE sample, while the second and third approach, which were not used here, considered a molar basis of plasticizer per mole of PE or moles of oxygen atoms in the plasticizer per mole of PE, respectively. Table 3.3 shows the plasticizer efficiency, determined on a mass basis, for biodiesel versus toluene averaged for the four grades of polyethylene. As seen in the table, k_{EM} for biodiesel was twice the value for toluene, indicating that biodiesel was more efficient as a plasticizer for polyethylene.

Table 3.3. Plasticizer efficiency of biodiesel versus toluene averaged for the four grades of polyethylene.

k_{EM} **(Biodiesel)**	k_{EM} **(Toluene)**

10.75 ± 1.66	5.73 ± 0.66

Although biodiesel demonstrated plasticization properties by traditional means of mechanical testing, the analysis using ultrasound indicated that its modes of interaction with the semi-crystalline structure of polyethylene are uniquely different from a plasticizer like toluene. Figures 3.3 and 3.4 show the different acoustic spectra attained from samples before and after immersion in biodiesel and toluene, respectively, where the weight gains were similarly around 2-4%.

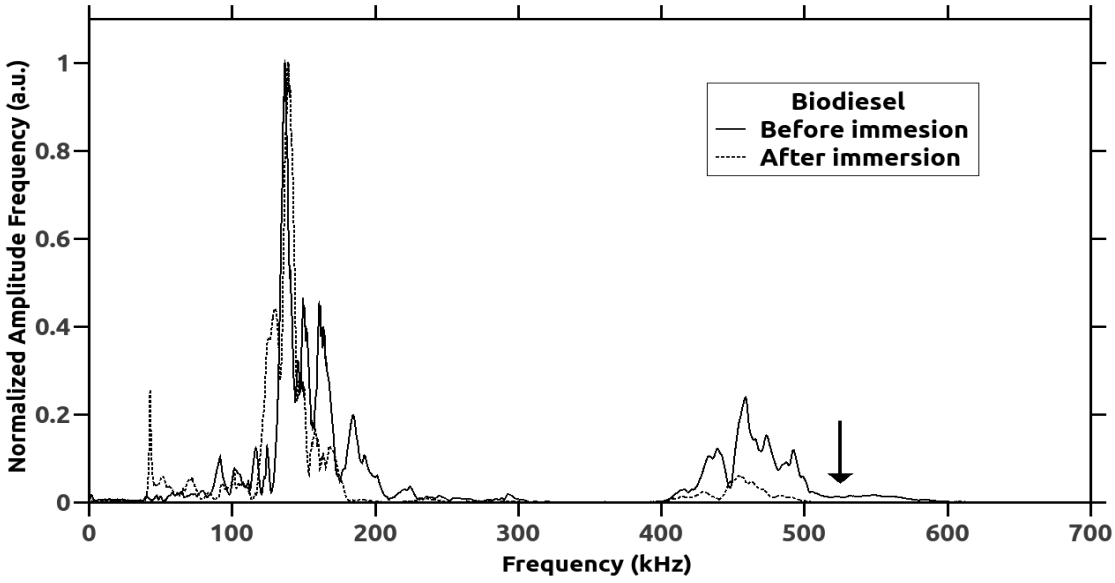

Figure 3.3. Ultrasonic spectra for the HD 8660.29 sample before and after biodiesel immersion (the arrow indicates the decrease of the third harmonic peak amplitude considering normalized signal based on primary frequency amplitude).

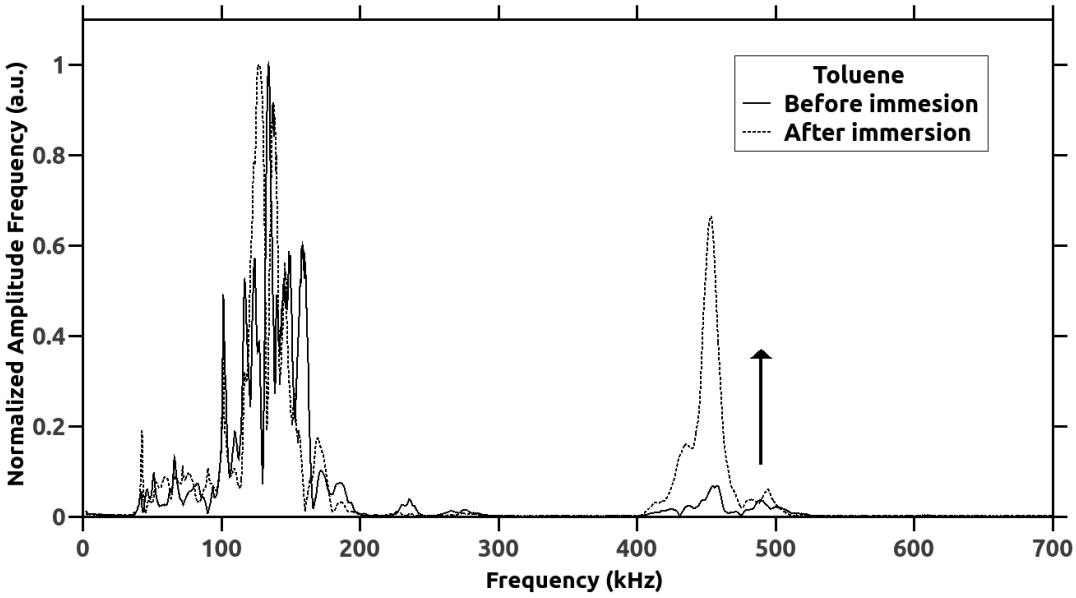

Figure 3.4. Ultrasonic spectra for the HD 8660.29 sample before and after toluene immersion (the arrow indicates the increase of the third harmonic peak amplitude considering normalized signal based on primary frequency amplitude).

The primary assumption of this analysis is that propagation of ultrasonic waves in PE will be dispersive, thus, presence of higher order harmonics will be detected. Unlike a perfect elastic body, propagation of these ultrasonic waves through a microstructure with discontinuities, such as those created in the semi-crystalline network with the penetration of solvents [27], can generate peaks at frequencies different from the original wave introduced. Experimental evidence has demonstrated that the observed harmonics is directly related with presence of non-linearities introduced in the structure of the material [31]. A distinct generation of third harmonic region (A3 – between 400-500 kHz) is observed in Figures 3.3 and 3.4. Second order and other higher order harmonic peaks were attenuated and thus not used for analysis. A descriptor used to quantify this difference is the amplitude ratio between the peaks of third harmonic (A3) and primary input frequency (A1), referred to as the ultrasonic parameter in this work. Variations in these ultrasonic

parameters are connected with structural changes that interfere with the nonlinear propagation of the ultrasonic waves. For PE plasticized by toluene, this region presented a significant increase in the ultrasonic parameter through an increase in the amplitude of the third harmonic region (A_3), while biodiesel caused a minor reduction (shown by the arrows in Figures 3.3 and 3.4). The changes in the ultrasonic parameter for all the samples following immersion in toluene and biodiesel were computed and plotted in Figure 3.5.

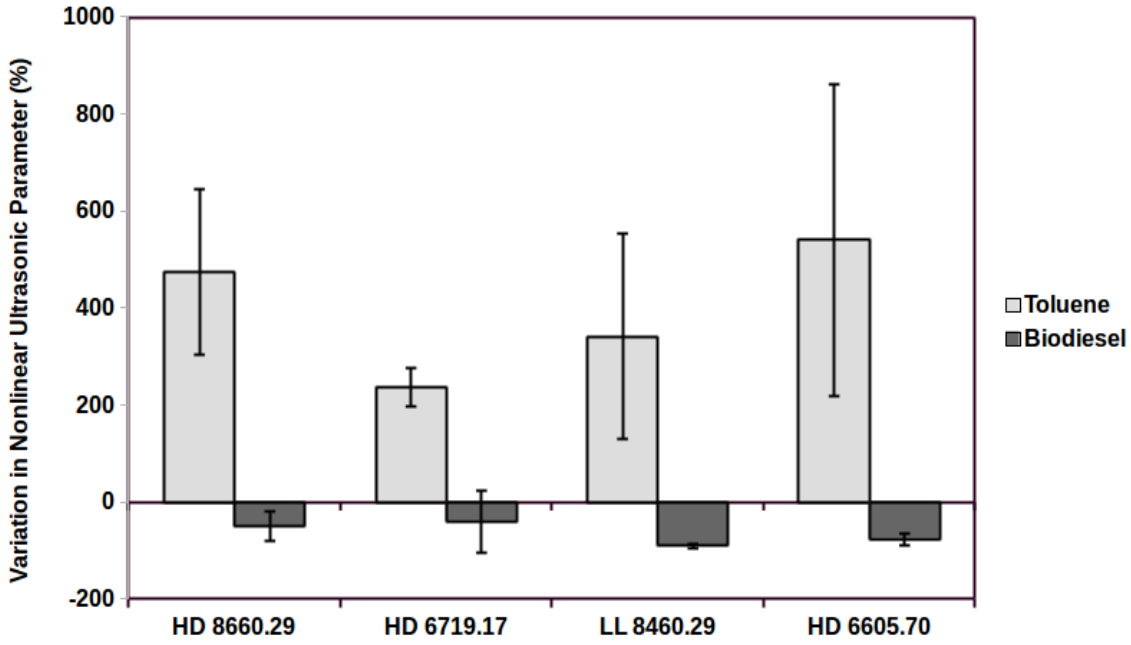

Figure 3.5. Nonlinear ultrasonic parameter variation for HD 8660.29, HD 6719.17, LL 8460.29, and HD 6605.70 with immersion in toluene and biodiesel.

When comparing the differences in the ultrasonic parameter, it is seen that the opposite behaviors in the third harmonics due to the influence of toluene or biodiesel was evident among all PE grades, with only a small difference attributed to crystallinity of the sample.

The interlamellar crystalline regions of the polymer samples are concentrated with stress transmitters spanning across the crystal lamellae boundaries, known as tie chains, which are associated with the mobility of the macromolecular network. These inter-crystalline regions can be affected by the penetration of low molecular weight contacting fluids, swelling the amorphous phase for polyethylene, and promoting internal stresses [32,33]. The increase in the nonlinear ultrasonic parameter occurred in response to increasing internal stress forces created by the penetrating molecules. Conversely, the decline in the nonlinear ultrasonic parameter shown in Figures 3.3 and 3.4, due to biodiesel absorption, is related to a relative decrease in internal stresses. This argument can be connected to observations of the necking regions during mechanical testing of these polyethylene samples after their immersion in the different plasticizers. Samples exposed to biodiesel exhibited a significant decrease in fibrillation while being stretched compared to those exposed to toluene. The absorbed biodiesel lubricated the inter-crystalline chains, similar to a stress-cracking agent, promoting crystal slippage during plastic deformation with no increase in internal stress. This was an interesting finding as it indicated the acoustic technique was differentiating the function of these two fluids with polyethylene in a manner not detectable by mechanical testing.

3.3.3. Effects of degradation of biodiesel on plasticization

Oxidative degradation of biodiesel results in chemical and physical changes to its properties, notable in its varying hydrophobicity and color, which may affect its absorption into polyethylene. Figure 3.6 presents the percent weight gains plotted against the time, from immersion in previously degraded biodiesel.

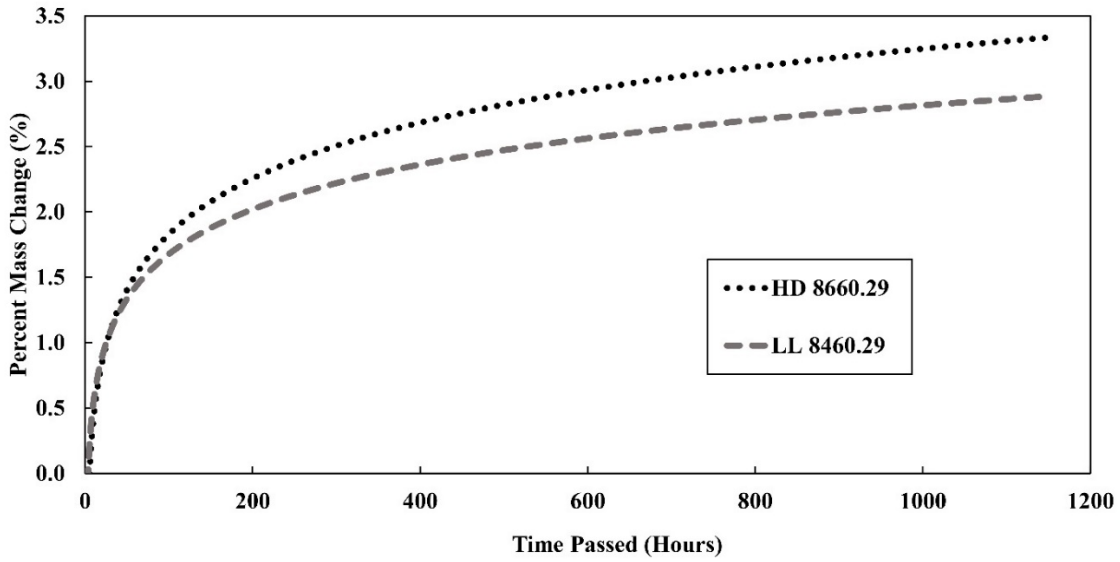

Figure 3.6. Plot of average percent weight change (%) vs. time passed (hours) of HD 8660.29 in degraded biodiesel (black dotted line), and LL 8460.29 in degraded biodiesel (gray dashed line). Experimental data points were fitted with a logarithmic curve. Experimental data points were fitted with a logarithmic curve. The average R^2 value for the two grades is 0.83 depicting a good correlation.

The plot shows no differences in the diffusion mechanism compared to fresh biodiesel (Figure 3.1) but the absorption rate was slightly lower with the degraded biofuel for LL 8460.29 and slightly higher for HD 8660.29. The LL 8460.29 samples in degraded biodiesel exhibited a percent mass change (2.89±0.06%) that was only 3.0% lower than fresh biodiesel whereas for the HD 8660.29 samples, the percent mass change (3.33±0.10%) was 9.53% lower.

The continued progression in oxidation during the immersion trials with both fresh biodiesel (Figure 3.1) and degraded biodiesel (Figure 3.6) was followed by determining the acid number and viscosity of the fluids over time; one must recognize that a fresh biodiesel sample experienced degradation as well in any such ageing studies since the antioxidants present in a commercial fuel will be consumed relatively quickly at 50 ^{o}C. Figure 3.7 shows the acid number

of both the degraded biodiesel and fresh biodiesel over time, reflecting changes in the concentration of acid groups formed as by-products of biodiesel ageing.

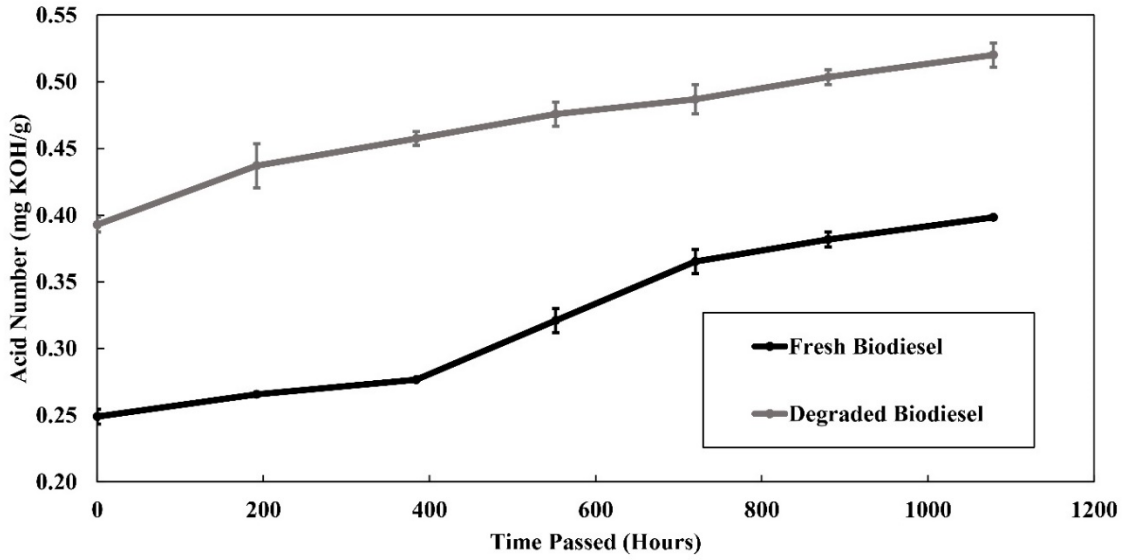

Figure 3.7. Plot of acid value vs. time passed for fresh biodiesel (black solid line) and degraded biodiesel (gray dashed line). Standard deviations, shown by the error bars, were higher with the degraded biodiesel due to the darker color making it more difficult to see the end point.

The two biofuels showed an 'almost constant' rate of increase in acid number even though the previously degraded biodiesel was always higher in value. The surface tension of fresh biodiesel, measured at Day 0, (25.95 ± 0.41 mN/m) was found to change very little from the 45-day degraded biodiesel (23.90 ± 0.34 mN/m). Acid groups were being increased in the fuel but the complex set of oxidation products related to degradation [34] meant the overall hydrophilicity was unchanged. On the other hand, the viscosity measurements showed no significant changes in the

viscosity of biodiesel over the degradation time, for either case, and consequently the data was not presented in the paper.

Mechanical testing found no significant differences between polyethylene samples plasticized by fresh versus degraded biodiesel, in terms of Young's Modulus or strain-at-max stress for both LL 8460.29 and HD 8660.29. The differences in biodiesel uptake between the fresh and degraded biodiesel were too small to have a detectable effect on the mechanical properties of the samples. Using Equation 2, the plasticization efficiency (k_{EM}) of the degraded biodiesel was found to be equal to 11.86 ± 1.35, which is not significantly different from that of fresh biodiesel (10.75 ± 1.66). In comparison, Figure 3.8 presents the variation of the nonlinear ultrasonic parameter for samples that were immersed in either fresh and degraded biodiesel.

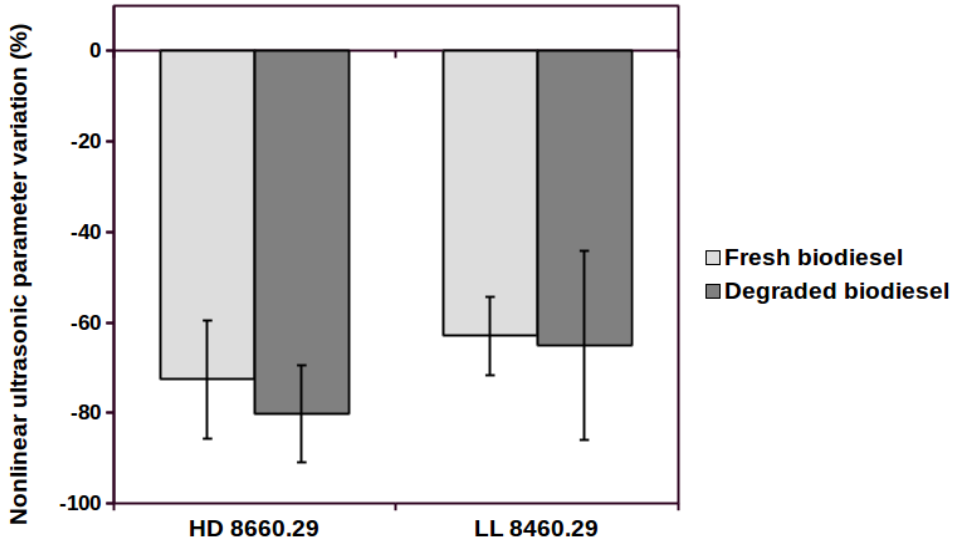

Figure 3.8. Nonlinear ultrasonic parameter variation for HD 8660.29 and LL 8460.29 with immersion in fresh and degraded biodiesel.

The results show that all samples experienced the same decrease in the variation of ultrasonic parameter after immersion but differences were too small to consider the degraded

biofuel to be affecting polyethylene differently. Since no significant difference was observed in both mechanical and ultrasonic tests, one concludes similar compatibility when using fresh and degraded biodiesel with polyethylene.

3.4. Conclusions

The compatibility assessment of biodiesel with polyethylene for use in fuel-contact service revealed a plasticizing property, though not as a swelling agent. Results from gravimetric analysis have noted a higher diffusivity coefficient (i.e. higher penetration rate) for biodiesel in polyethylene samples of lower density (i.e. lower crystallinity). Immersion of the same samples in toluene showed a slightly different absorption behavior and higher diffusion rates in comparison to biodiesel. The effect of biodiesel and toluene sorption on the mechanical properties (Young's Modulus) of polyethylene showed significantly higher plasticization efficiencies for biodiesel in comparison to toluene. A novel non-destructive testing method based on ultrasonics was used to evaluate biodiesel plasticization (in comparison to toluene). Differences in the resulting acoustic signature expressed by biodiesel and toluene revealed interesting evidence of different modes of interaction (plasticization) with the semi-crystalline structure of polyethylene between the two fluids, that was not detectable by the mechanical testing. An increase in the nonlinear ultrasonic parameter is witnessed by the toluene plasticized samples as a result of increasing internal stress forces created by the penetrating molecules. Conversely, a decline in the nonlinear ultrasonic parameter is witnessed in the biodiesel plasticized samples in relation to a relative decrease in internal stresses. Oxidation of biodiesel by degradation was found to only slightly affect the diffusion rate of biodiesel into polyethylene samples, though mechanical and ultrasonic testing showed no significant differences in the plasticization capability of biodiesel.

Future studies by our group will concentrate on attaining a deeper understanding of the

compatibility of biodiesel and polyethylene, specifically the accelerated failures that can occur upon exposure of the small stresses.

Acknowledgements

The authors would like to thank Imperial Oil Ltd., Natural Sciences and Engineering Research Council (NSERC), and the Conselho Nacional de Desenvolvimento Científico e Tecnológico (CNPq) for funding the work. The authors would like to especially thank Ron Cooke at Imperial Oil for his advice, supply of materials, and technical insights.

References

[1] O.-G. Piringer, A.L. Baner, Plastic packaging: interactions with food and pharmaceuticals, Wiley-VCH, Weinheim, 2008.

[2] W. Trakarnpruk, S. Porntangjitlikit, Palm oil biodiesel synthesized with potassium loaded calcined hydrotalcite and effect of biodiesel blend on elastomer properties, Renewable Energy. 33 (2008) 1558–1563. doi:10.1016/j.renene.2007.08.003.

[3] B. Flitney, Which elastomer seal materials are suitable for use in biofuels?, Sealing Technology. 2007 (2007) 8–11. doi:10.1016/s1350-4789(07)70409-9.

[4] E. Richaud, Flaconnèche Bruno, J. Verdu, Biodiesel permeability in polyethylene, Polymer Testing. 31 (2012) 170–1076. doi:10.1063/1.4738433.

[5] M. Böhning, U. Niebergall, A. Adam, W. Stark, Influence of biodiesel sorption on temperature-dependent impact properties of polyethylene, Polymer Testing. 40 (2014) 133–142. doi:10.1016/j.polymertesting.2014.09.001.

[6] M. Schilling, M. Böhning, H. Oehler, I. Alig, U. Niebergall, Environmental stress cracking of polyethylene high density (PE-HD) induced by liquid media - Validation and verification of the full-notch creep test (FNCT), Materialwissenschaft Und Werkstofftechnik. 48 (2017) 846–854. doi:10.1002/mawe.201700065.

[7] M.M. Maru, M.M. Lucchese, C. Legnani, W.G. Quirino, A. Balbo, I.B. Aranha, et al., Biodiesel compatibility with carbon steel and HDPE parts, Fuel Processing Technology. 90 (2009) 1175–1182. doi:10.1016/j.fuproc.2009.05.014.

[8] M. Böhning, U. Niebergall, A. Adam, W. Stark, Impact of biodiesel sorption on mechanical properties of polyethylene, Polymer Testing. 34 (2013) 17–24. doi:10.1016/j.polymertesting.2013.12.003.

[9] M. Böhning, U. Niebergall, M. Zanotto, V. Wachtendorf, Impact of biodiesel sorption on tensile properties of PE-HD for container applications, Polymer Testing. 50 (2016) 315–324. doi:10.1016/j.polymertesting.2016.01.025.

[10] M. Weltschev, J. Werner, M. Haufe, M. Heyer, Compatibility of High-Density Polyethylene Grades with Biofuels, Packaging Technology and Science. 27 (2013) 231–240. doi:10.1002/pts.2028.

[11] M. Thompson, B. Mu, C. Ewaschuk, Y. Cai, K. Oxby, J. Vlachopoulos, Long term storage of biodiesel/petrol diesel blends in polyethylene fuel tanks, Fuel. 108 (2013) 771–779. doi:10.1016/j.fuel.2013.02.040.

[12] G. Lutz, J.F. Mata-Segreda, Kinetics of interaction of palm ethyl biodiesel with three different polymer materials, Journal of Physical Organic Chemistry. 21 (2008) 1068–1071. doi:10.1002/poc.1427.

[13] H.J. Nieschlag, I.A. Wolff, Industrial uses of high erucic oils, Journal of the American Oil Chemists Society. 48 (1971) 723–727. doi:10.1007/BF02638529

[14] P.P. Kundu, Improvement of filler-rubber interaction by the coupling action of vegetable oil in carbon black reinforced rubber, Journal of Applied Polymer Science. 75 (1999) 735–739. doi:10.1002/(sici)1097-4628(20000207)75:6<735::aid-app1>3.0.co;2-t.

[15] V. Nandanan, R. Joseph, K.E. George, Rubber seed oil: A multipurpose additive in NR and SBR compounds, Journal of Applied Polymer Science. 72 (1999) 487–492. doi:10.1002/(sici)1097-4628(19990425)72:4<487::aid-app4>3.0.co;2-m.

[16] J. Wehlmann, Use of esterified rapeseed oil as plasticizer in plastics processing, Lipid - Fett. 101 (1999) 249–256. doi:10.1002/(sici)1521-4133(199907)101:7<249::aid-lipi249>3.0.co;2-i.

[17] F. Cataldo, O. Ursini, G. Angelini, Biodiesel as a Plasticizer of a SBR-Based Tire Tread Formulation, ISRN Polymer Science. 2013 (2013) 1–9. doi:10.1155/2013/340426.

[18] R. Mccormick, M. Ratcliff, L. Moens, R. Lawrence, Several factors affecting the stability of biodiesel in standard accelerated tests, Fuel Processing Technology. 88 (2007) 651–657. doi:10.1016/j.fuproc.2007.01.006.

[19] M. Fazal, A. Haseeb, H. Masjuki, Biodiesel feasibility study: An evaluation of material compatibility; performance; emission and engine durability, Renewable and Sustainable Energy Reviews. 15 (2011) 1314–1324. doi:10.1016/j.rser.2010.10.004.

[20] M. Jakeria, M. Fazal, A. Haseeb, Influence of different factors on the stability of biodiesel: A review, Renewable and Sustainable Energy Reviews. 30 (2014) 154–163. doi:10.1016/j.rser.2013.09.024.

[21] E. Richaud, B. Fayolle, J. Verdu, J. Rychlý, Co-oxidation kinetic model for the thermal oxidation of polyethylene-unsaturated substrate systems, Polymer Degradation and Stability. 98 (2013) 1081–1088. doi:10.1016/j.polymdegradstab.2013.01.008.

[22] E. Richaud, F. Djouani, B. Fayolle, J. Verdu, B. Flaconneche, New Insights in Polymer-Biofuels Interaction, Oil & Gas Science and Technology – Revue d'IFP Energies Nouvelles. 70 (2013) 317–333. doi:10.2516/ogst/2013151.

[23] N. Lützow, A. Tihminlioglu, R.P. Danner, J. Duda, A.D. Haan, G. Warnier, et al., Diffusion of toluene and n-heptane in polyethylenes of different crystallinity, Polymer. 40 (1999) 2797–2803. doi:10.1016/s0032-3861(98)00473-x.

[24] R. Kwamen, B. Blümich, A. Adams, Estimation of Self-Diffusion Coefficients of Small Penetrants in Semicrystalline Polymers Using Single-Sided NMR, Macromolecular Rapid Communications. 33 (2012) 943–947. doi:10.1002/marc.201100847.

[25] D. Cava, R. Catala, R. Gavara, J.M. Lagaron, Testing limonene diffusion through food contact polyethylene by FT-IR spectroscopy: Film thickness, permeant concentration and outer medium effects, Polymer Testing. 24 (2005) 483–489. doi:10.1016/j.polymertesting.2004.12.003.

[26] M. Wang, P. Wu, S.S. Sengupta, B.I. Chadhary, J.M. Cogen, B. Li, Investigation of Water Diffusion in Low-Density Polyethylene by Attenuated Total Reflectance Fourier Transform Infrared Spectroscopy and Two-Dimensional Correlation Analysis, Industrial & Engineering Chemistry Research. 50 (2011) 6447–6454. doi:10.1021/ie102221a.

[27] F. Gomes, W. West, M. Thompson, Effects of annealing and swelling to initial plastic deformation of polyethylene probed by nonlinear ultrasonic guided waves, Polymer. 131 (2017) 160–168. doi:10.1016/j.polymer.2017.10.041.

[28] M.H. Cohen, D. Turnbull, Molecular Transport in Liquids and Glasses, The Journal of Chemical Physics. 31 (1959) 1164–1169. doi:10.1063/1.1730566.

[29] M. Bocqué, C. Voirin, V. Lapinte, S. Caillol, J.-J. Robin, Petro-based and bio-based plasticizers: Chemical structures to plasticizing properties, Journal of Polymer Science Part A: Polymer Chemistry. 54 (2015) 11–33. doi:10.1002/pola.27917.

[30] R. Sothornvit, J.M. Krochta, Plasticizer effect on mechanical properties of β-lactoglobulin films, Journal of Food Engineering. 50 (2001) 149–155. doi:10.1016/s0260-8774(00)00237-5.

[31] C.J. Lissenden, Y. Liu, J.L. Rose, Use of non-linear ultrasonic guided waves for early damage detection, Insight - Non-Destructive Testing and Condition Monitoring. 57 (2015) 206–211. doi:10.1784/insi.2015.57.4.206.

[32] A. Krajenta, A. Rozanski, R. Idczak, Morphology and properties alterations in cavitating and non-cavitating high density polyethylene, Polymer. 103 (2016) 353–364. doi:10.1016/j.polymer.2016.09.068.

[33] A. Rozanski, A. Galeski, Plastic yielding of semicrystalline polymers affected by amorphous phase, International Journal of Plasticity. 41 (2013) 14–29. doi:10.1016/j.ijplas.2012.07.008.